

## Enhancing the magnetoelectric coupling in YMnO<sub>3</sub> by Ga doping

A. A. Nugroho,<sup>1,2</sup> N. Bellido,<sup>3</sup> U. Adem,<sup>1</sup> G. Nénert,<sup>1</sup> Ch. Simon,<sup>3</sup> M. O. Tjia,<sup>2</sup> M. Mostovoy,<sup>1,4</sup> and T. T. M. Palstra<sup>1</sup>

<sup>1</sup>Materials Science Center, University of Groningen, 9747 AG Groningen, The Netherlands

<sup>2</sup>Faculty of Mathematics and Natural Sciences, Institut Teknologi Bandung, Jl. Ganesha 10, Bandung 40132, Indonesia

<sup>3</sup>Laboratoire CRISMAT, UMR CNRS ENSICAEN, 1450 Caen, France

<sup>4</sup>II. Physikalisches Institut, University of Cologne, 50937 Cologne, Germany

(Received 17 October 2006; revised manuscript received 23 March 2007; published 24 May 2007)

We study the magnetoelectric coupling in YMnO<sub>3</sub> single crystal, in which a part of Mn<sup>3+</sup> ions is substituted by nonmagnetic Ga<sup>3+</sup> ions. While the antiferromagnetic ordering temperature is gradually suppressed by Ga doping, the magnetocapacitance is enhanced by two orders of magnitude, which we attribute to the lifting of frustration of interlayer spin interactions in doped samples. We also find that the dielectric constant anomaly below magnetic ordering temperature is strongly anisotropic, which we explain using a phenomenological Landau description of ferroelectric antiferromagnets.

DOI: [10.1103/PhysRevB.75.174435](https://doi.org/10.1103/PhysRevB.75.174435)

PACS number(s): 75.80.+q, 77.80.-e, 77.84.-s

The unusual coexistence of spontaneous electric polarization with low-dimensional magnetic ordering observed in hexagonal manganites, h-RMnO<sub>3</sub>, has triggered intensive studies and explorations of multiferroic materials.<sup>1</sup> An important parameter in these materials is the coupling strength between electric polarization and magnetization, which enables the control of electric (magnetic) properties by applied magnetic (electric) fields.<sup>2,3</sup> The magnetoelectric coupling in YMnO<sub>3</sub> gives rise to clamping of ferroelectric and antiferromagnetic domains observed in nonlinear dielectric susceptibility measurements, the anomalies of the dielectric constant at magnetic transitions,<sup>4-6</sup> and the strong scattering of acoustic phonons by magnetic fluctuations observed in thermal conductivity measurements.<sup>7</sup>

YMnO<sub>3</sub> belongs to the class of h-RMnO<sub>3</sub> compounds with *R* denoting a small-radius rare-earth ion from Ho to Lu and *Y*. Hexagonal manganites become ferroelectric at  $T_C \approx 900$  K with the spontaneous polarization occurring along the *c* direction. Although exchange interactions between the magnetic Mn<sup>3+</sup> ions are relatively strong, as implied by the high Curie-Weiss temperatures around 700 K,<sup>5</sup> the antiferromagnetic ordering of Mn<sup>3+</sup> spins with triangular structure in these materials generally occurs in both polycrystal<sup>8</sup> and single-crystal<sup>9</sup> samples at a much lower temperature of  $T_N \approx 70$  K. This is partly a consequence of the quasi-two-dimensional magnetic structure of h-RMnO<sub>3</sub> where Mn spins form weakly coupled layers in the *ab* basal plane. Further, each layer has a triangular structure, in which the nearest-neighbor spins are coupled antiferromagnetically, resulting in magnetic frustration of both intra- and interlayer exchange interactions.

The coupling between electric and magnetic phenomena in these materials is not very strong, which is related to different origins of ferroelectricity and magnetism and the resulting large difference between the ferroelectric and spin ordering temperatures. In this respect, hexagonal manganites are very different from orthorhombic RMnO<sub>3</sub> compounds, where ferroelectricity is induced by magnetic ordering.<sup>10-12</sup>

In this paper, we report the strong enhancement of the magnetoelectric coupling observed in Ga-doped h-YMnO<sub>3</sub>. A previous study showed that Ga doping does not strongly affect ferroelectricity in YMnO<sub>3</sub>; the ferroelectric transition

temperature only slightly increases upon Ga substitution.<sup>13</sup> Here, we show that the effect of the substitution on the magnetoelectric coupling is much more dramatic. In ferroelectric antiferromagnets, one should distinguish between the coupling of the electric polarization *P* to the Néel order parameter *L*, which gives rise to an anomaly of the dielectric susceptibility at the magnetic transition, and the coupling of *P* to the uniform magnetic field *H*, which gives rise to magnetocapacitance. While the former coupling is not strongly affected by Ga substitution, the coupling of the electric polarization along the *c* direction to a uniform magnetic field increases by two orders of magnitude upon 30% Ga doping. The substitution of nonmagnetic Ga for Mn suppresses the antiferromagnetic ordering by diluting the magnetic system. Therefore, the observed increase of magnetocapacitance is likely related to a change of magnetic ordering upon doping.

Single crystals of YMn<sub>1-x</sub>Ga<sub>x</sub>O<sub>3</sub> with *x*=0.0, 0.1, 0.3, and 0.5 were grown using the floating zone technique. The crystallinity of the as-grown rods was checked by Laue diffraction. Single-crystal x-ray diffraction was carried out using an APEX Bruker, equipped with a charge-coupled device detector at 296 and 100 K. The data were refined using SHELXL, yielding Ga concentrations of *x*=0.0, 0.1, 0.28, and 0.51, which are close to the nominal compositions. We will use the refinement results at 100 K, which have better resolution than those at 296 K.<sup>14</sup> The magnetization was measured on the oriented samples using a superconducting quantum interference device magnetometer (MPMS of Quantum Design). For the dielectric measurements, the crystals were oriented along the *b* and *c* axes (denoted as  $\perp c$  and  $\parallel c$ ) and cut into a typical cross section of  $4 \times 3$  mm<sup>2</sup> and thickness of 0.5 mm. The surfaces were polished and covered with Ag paste. The electrical contacts were made using Pt wire connected to the surface by additional Ag paste. The capacitance was measured using an Andeen-Hagerling AH2500A capacitance bridge operating at a fixed frequency of 1 kHz for *H* in the range  $\leq 8$  T. For the high-field measurement in the range of  $H \leq 14$  T, the electric contacts were made by copper wire with indium paste using ultrasonic method, while the capacitance was measured by an Agilent AG4284A LCR meter. The samples were mounted on a homemade insert for the PPMS temperature platform of Quantum Design. A systematic

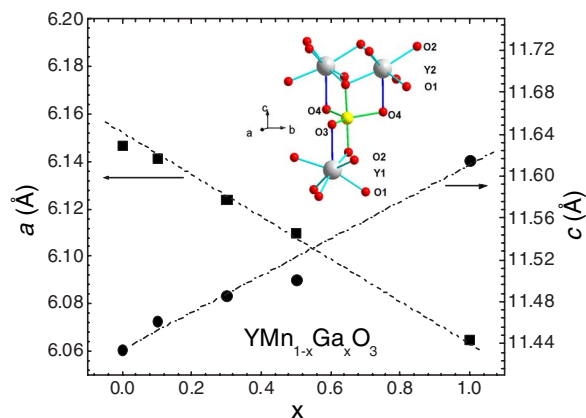


FIG. 1. (Color online) Variations of lattice parameters vs of Ga dopant concentration in  $\text{YMnO}_3$  single crystals. The lines are guides to the eyes

check of the amplitude and frequency dependence ruled out any “extrinsic” effects. The dielectric constant was extracted from the capacitance using the sample and/or contact dimensions for  $x=0$ , neglecting edge corrections.

The changes of the lattice parameters with increasing Ga substitution are shown in Fig. 1. The lattice parameter  $a$  decreases whereas  $c$  increases monotonically with increasing substitution.<sup>13,14</sup> This is to be expected because the atomic radius of  $\text{Ga}^{3+}$  (0.69 Å) is smaller than that of  $\text{Mn}^{3+}$  (0.72 Å), and Ga ( $d^{10}$ ) doping fills the  $d_{3z^2-r^2}$  orbital, which is empty for  $\text{Mn}^{3+}$  ions in bipyramidal oxygen coordination. The ferroelectric state of  $\text{YMnO}_3$  is usually associated with a shortening and/or elongation of relative distance between O3(O4) and Y1(Y2) along the  $c$  axis.<sup>15</sup> As shown in Fig. 1, the nearest neighbors of Y1(Y2) are not O3(O4), but the apical oxygens O1(O2) of the  $\text{MnO}_5$  bipyramids. The largest contribution to the local dipole moments actually originates from the O1(O2) ions, which coordinate Y1 and Y2 as an antiprism. The local dipole moment of the  $\text{Y1O}_6$  and  $\text{Y2O}_6$  antiprisms decreases slightly (<10%) with Ga substitution.<sup>14</sup> Despite these displacements, the position of Mn/Ga atom remains close to the barycenter of the bipyramids.<sup>15</sup> We found from our single-crystal refinements no significant change in the tilting and buckling of the  $\text{MnO}_5$  bipyramids upon Ga substitution, despite the change induced in the  $c/a$  ratio. In addition to the displacements responsible for the ferroelectricity, additional displacements of about 1% were observed in Mn–O3 and the Mn–O4 bond lengths below the magnetic transition.<sup>16,17</sup>

In order to relate the structural changes with the magnetic behavior, we have measured the temperature dependence of the magnetization of  $\text{Y}(\text{Mn},\text{Ga})\text{O}_3$  for  $H\parallel c$  and  $H\perp c$  (see Fig. 2). The magnetic ordering transitions marked by cusps on the susceptibility curves were clearly observed up to  $x=0.3$  in a magnetic field applied along the  $c$  axis. We further note that for low substitution ( $x=0.1$ ), the magnetic anisotropy and temperature dependence of the susceptibility are similar to those in the undoped compound,<sup>5</sup> whereas for  $x=0.3$ , the magnetic transition is observed only in a magnetic field along the  $c$  axis. The Néel temperature decreases from 72 K for  $x=0$  to 65 K for  $x=0.1$  and to 35 K for  $x=0.3$ , as

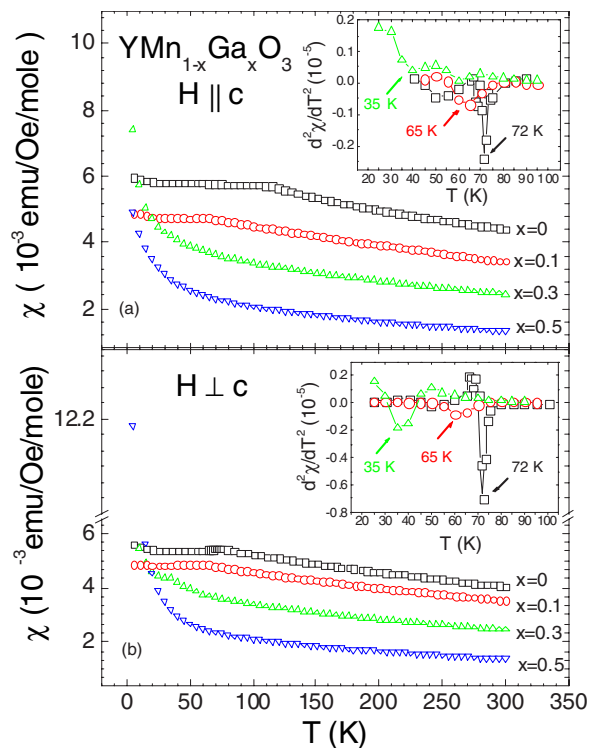


FIG. 2. (Color online) Temperature dependence of magnetization measured in magnetic field of 1000 Oe from Ga-substituted  $\text{YMnO}_3$  single crystals for (a)  $H\perp c$  and (b)  $H\parallel c$ . The insets show the Néel temperatures obtained from the minimum of  $d^2\chi/dT^2$ .

shown in Fig. 2. Also, the magnitude of Curie-Weiss temperature  $T_{CW}$  decreases with increasing Ga concentration:  $T_{CW}=-567$  K for  $x=0$ ,  $-547$  K for  $x=0.1$ ,  $-531$  K for  $x=0.3$ , and  $-501$  K for  $x=0.5$ . The corresponding effective moments per  $\text{Mn}^{3+}$  are  $4.93\mu_B$  for  $x=0.0$ ,  $4.82\mu_B$  for  $x=0.1$ ,  $4.38\mu_B$  for  $x=0.3$ , and  $3.62\mu_B$  for  $x=0.5$ . Thus, the ratio of  $|T_{CW}|$  to  $T_N$ , indicative of frustration in the magnetic structure, increases upon doping.

Figure 3 shows the temperature dependence of the capacitance  $C(T)$  for (a)  $E\perp c$  and (b)  $E\parallel c$ . The changes in the capacitance are much larger than those expected from thermal expansion and possible sample size change due to magnetostriction effect, which has been shown to yield less than 0.1% sample size change in rare-earth based antiferromagnets.<sup>18</sup> The observed variation should therefore reflect the temperature dependence of the dielectric constant  $\epsilon$ . The onset of magnetoelectric coupling indicated by the sudden drop of capacitance is clearly observed at the corresponding Néel temperatures up to 30% Ga doping for  $E\perp c$ , but is only barely visible for  $E\parallel c$  in the undoped compound. Although the anomalies of dielectric constant at the magnetic transition are not as large as those observed in orthorhombic manganites, the fact that the in-plane dielectric constant displays much more sensitive response to the presence of antiferromagnetic order than the uniform magnetic susceptibility is itself a remarkable property of hexagonal manganites.<sup>19,20</sup>

The inset of Fig. 3 shows the influence of antiferromagnetic order  $L$  on  $\epsilon$ , obtained from the capacitance data by subtracting the extrapolated high-temperature data, fitted

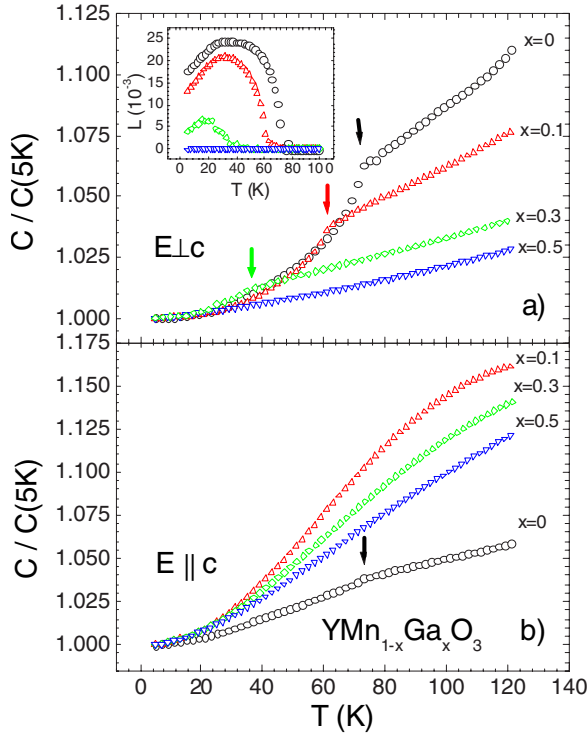


FIG. 3. (Color online) Temperature dependence of the capacitance of Ga-doped  $\text{YMnO}_3$  single crystals normalized at 5 K for (a)  $E \perp c$  and for (b)  $E \parallel c$ .

with  $C(T) = AT^2$ . Assuming that the capacitance anomaly  $\Delta C \propto L^2$  below the magnetic transition, the magnetic order parameter can be fitted by  $L(T) = L_0(1 - T/T_N)^\beta$ , with  $\beta = 0.33, 0.39,$  and  $0.43$  for  $x = 0, 0.1,$  and  $0.3$ , respectively. These values are reasonably close to  $\beta = 0.37$  for a three-dimensional Heisenberg model.<sup>21</sup> We also note that Ga substitution suppresses the temperature variation of  $\epsilon$  in both orientations, except for  $\epsilon_{\parallel}$ , which undergoes a large increase from  $x = 0.0$  to  $0.1$ .

Figure 4 shows the magnetic-field dependence of the capacitance for  $E \perp c$  [panel (a)] and  $E \parallel c$  [panel (b)], measured for the pure and 30% Ga-substituted crystals at 5 K. In both cases, the capacitance varies quadratically with an applied magnetic field. For  $x = 0$ , the anisotropy of the magnetocapacitance is similar to that of the dielectric constant at  $T_N$ , exhibiting a stronger magnetic-field dependence of  $\epsilon_{\perp}$  compared to  $\epsilon_{\parallel}$ . This large difference in the in-plane and out-of-plane magnetodielectric response is to a large extent the consequence of the anisotropy of  $\epsilon$  itself, which can be understood by considering thermodynamic potential of a ferroelectric antiferromagnet:

$$\begin{aligned} \Phi = & \Phi_{\text{FE}}(\mathbf{P}) + \Phi_{\text{AFM}}(\mathbf{L}) - \mathbf{E} \cdot \mathbf{P} + \frac{1}{2}[g_{\perp}(P_a^2 + P_b^2) + g_{\parallel}P_c^2]L^2 \\ & + \frac{1}{2}[\gamma_{\perp}(P_a^2 + P_b^2) + \gamma_{\parallel}P_c^2]H^2 + \frac{1}{2}[-\chi_m^{(0)}H^2 + c_1L^2H^2 \\ & + c_2(\mathbf{L} \cdot \mathbf{H})^2]. \end{aligned} \quad (1)$$

In this equation, the first two terms describe the ferroelectric

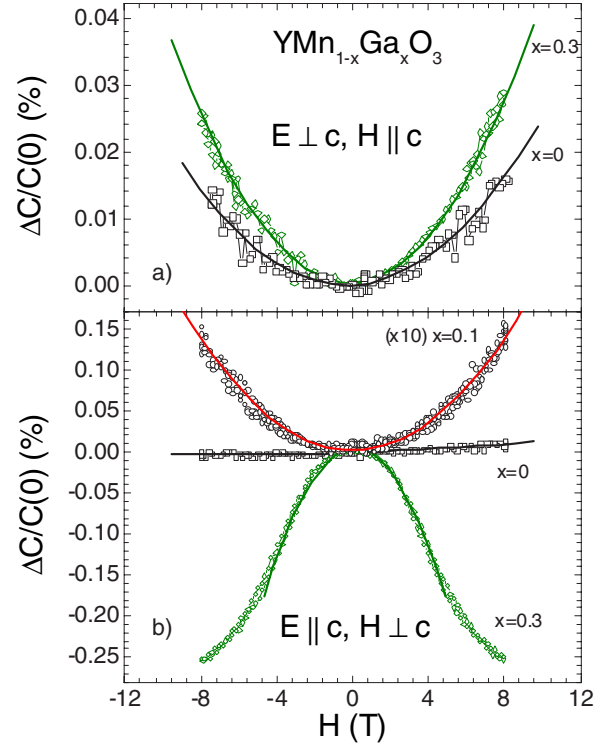


FIG. 4. (Color online) Magnetocapacitance at 5 K of  $\text{YMnO}_3$  with 30% Ga doping for (a)  $E \perp c$  and  $H \parallel c$ , (b)  $E \parallel c$ , and  $H \perp c$ .

and magnetic subsystems, the third term denotes the coupling to electric field, the fourth term describes the coupling between the ferroelectric order parameter  $\mathbf{P}$  and the antiferromagnetic order parameter  $\mathbf{L}$  with the in-plane and out-of-plane magnetoelectric coupling strengths  $g_{\perp}$  and  $g_{\parallel}$ , and the fifth term is the coupling between  $\mathbf{P}$  and a uniform magnetic field  $\mathbf{H}$ . Finally, the last term describes the coupling of the antiferromagnet to magnetic field. The ferroelectric subsystem, described by Eq. (1), has a uniaxial anisotropy, while magnetic anisotropies in  $\text{Y}_{1-x}\text{Ga}_x\text{MnO}_3$  are weak, as shown in Figs. 5(a) and 5(b), respectively.

In Fig. 6, we show the magnetocapacitance and magnetization up to 14 T for  $x = 0$ . We notice that the capacitance obeys a quadratic magnetic-field dependence, originating from the  $P^2H^2$  coupling and corresponding to linear increase of magnetization with increasing field. Figure 5 shows that this behavior changes upon substitution. For  $x = 0.3$ , deviations from  $C(H) \sim H^2$  and  $M(H) \sim H$  set in above 4 T. For higher magnetic fields, the magnetization starts to saturate, which is reflected in saturation of the magnetocapacitance. Nevertheless, both systems exhibit little magnetic anisotropy, and thus while the (magneto)capacitance is anisotropic, the magnetization itself is not very sensitive to the direction of the magnetic field.

To first order in the coupling constants, the change of the longitudinal and transversal dielectric susceptibilities  $\chi_{\parallel}$  and  $\chi_{\perp}$  in the presence of antiferromagnetic ordering and an applied magnetic field can be written as  $\Delta\chi_{\parallel} = \chi_{\parallel}(L, H) - \chi_{\parallel}(0, 0) \approx -\chi_{\parallel}^{(0)}(g_{\parallel}L^2 + \gamma_{\parallel}H^2)$  and  $\Delta\chi_{\perp} \approx -\chi_{\perp}^{(0)}(g_{\perp}L^2 + \gamma_{\perp}H^2)$ . Thus, their ratio becomes

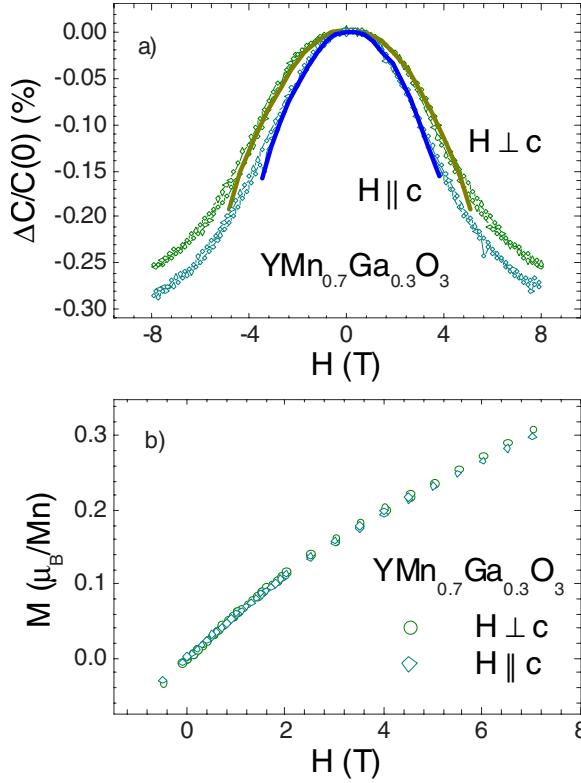


FIG. 5. (Color online) (a) Magnetocapacitance effect of 30% Ga doping level of  $\text{YMnO}_3$  at 5 K for  $E \parallel c$  in magnetic field applied along  $H \parallel c$  and  $H \perp c$ ; (b) field dependence of magnetization for  $x=0.3$  with magnetic field applied along  $H \parallel c$  and  $H \perp c$ .

$$R = \frac{\Delta \varepsilon_{\perp}}{\Delta \varepsilon_{\parallel}} \approx \left( \frac{\varepsilon_{\perp} - 1}{\varepsilon_{\parallel} - 1} \right)^2 \left( \frac{g_{\perp} L^2 + \gamma_{\perp} H^2}{g_{\parallel} L^2 + \gamma_{\parallel} H^2} \right). \quad (2)$$

Since for  $\text{YMnO}_3$  the dielectric constant  $\varepsilon_{\perp} \approx 21$  (transverse to the direction of the spontaneous polarization) is significantly larger than the longitudinal dielectric constant  $\varepsilon_{\parallel} \approx 5$ , the ratio of anomalies at  $T_N$  is  $R \approx 25 g_{\perp} / g_{\parallel}$ , while the ratio of magnetocapacitances is  $R \approx 25 \gamma_{\perp} / \gamma_{\parallel}$ . An additional source of magnetoelectric response is the quasi-two-dimensional magnetic structure of  $\text{YMnO}_3$ : one expects that  $g_{\perp} > g_{\parallel}$  and  $\gamma_{\perp} > \gamma_{\parallel}$ , as these coupling constants scale with the spin-exchange couplings in the corresponding directions.

Most interestingly, the magnetocapacitance of this material shows a strong dependence on Ga doping. We observe an approximately twofold increase in the transverse magnetoelectric coupling: from  $\gamma_{\perp} = -31 \times 10^{-4} \text{ T}^{-2}$  for  $x=0$  to  $\gamma_{\perp} = -55 \cdot 10^{-4} \text{ T}^{-2}$  for  $x=0.3$  [see Fig. 4(a)]. However, a much more pronounced increase of approximately two orders of magnitude is shown in Fig. 4(b) for the coupling along the  $c$  axis: from  $\gamma_{\parallel} = -11 \times 10^{-4} \text{ T}^{-2}$  for  $x=0$  to  $\gamma_{\parallel} = 14 \times 10^{-2} \text{ T}^{-2}$  for  $x=0.3$  accompanied by a sign reversal of magnetoelectric coupling constant  $\gamma_{\parallel}$ . While in the undoped sample  $\gamma_{\parallel}$  is comparable to  $\gamma_{\perp}$  and the anisotropy of the magnetocapacitance largely reflects the anisotropy of the dielectric constant [see Eq. (2)], its value for  $x=0.3$  doping is clearly two orders of magnitude larger than  $\gamma_{\perp}$ , so that the relative change of capacitance in magnetic field becomes larger for  $E \parallel c$ .

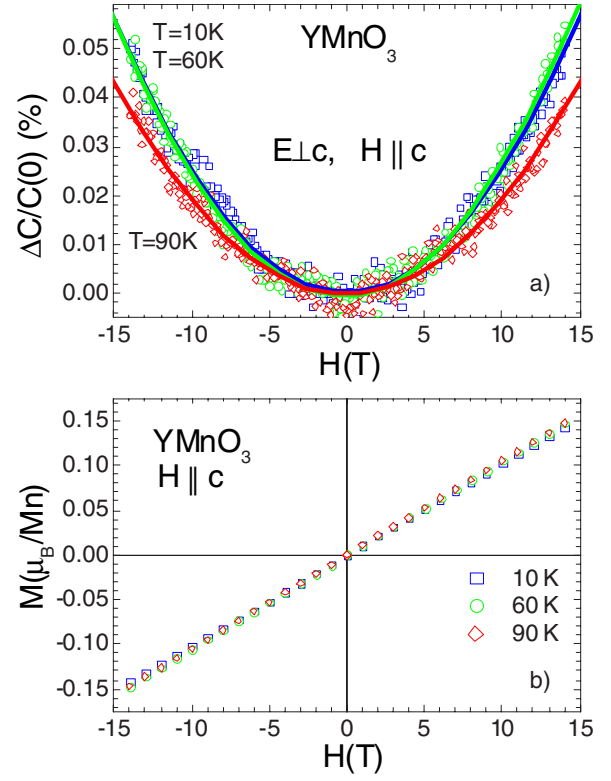


FIG. 6. (Color online) (a) Magnetic-field dependence of in-plane dielectric constant at 10, 60, and 90 K. (b) Magnetization of  $\text{YMnO}_3$  along the  $c$ -axis function of magnetic field at 10, 60, and 90 K.

The coupling of electric polarization to magnetic field can be mediated by a phonon or a strain.<sup>22</sup> If, for example,  $P$  and  $H$  are coupled to a lattice distortion of the amplitude  $u$  by  $\Phi_{int} = -u(\alpha P^2 + \beta H^2)$ , then minimization of the sum of  $\Phi_{int}$  and the lattice energy  $\frac{K}{2}u^2$  with respect to  $u$  gives (among other terms) an effective coupling  $\frac{1}{2}\gamma P^2 H^2$  with  $\gamma = -\frac{2\alpha\beta}{K}$ . The increase of  $\gamma$  upon doping then reflects the increase of the coupling constants  $\alpha$  or/and  $\beta$ . While our measurements do not allow us to make definite conclusions, the observed enhancement of magnetocapacitance is likely related to an increase of lattice distortion in an applied magnetic field, as the  $120^\circ$  spin state is suppressed by doping.

The magnetoelastic coupling in hexagonal  $\text{RMnO}_3$  is known to be rather strong.<sup>20,23</sup> However, the interlayer spin exchange in the  $120^\circ$  state, sensitive to shifts of ions in the  $c$  direction, is strongly frustrated, as each spin is coupled to three spins forming a triangle in a neighboring layer, which add up to zero total spin. Similar temperature dependence of dielectric and magnetic susceptibilities of clean and doped samples shows that at least up to  $x=0.3$ , the spin dilution does not fully suppress magnetic ordering and does not give rise to a spin-glass state, as observed in some other frustrated materials. Rather, the initial quasi-two-dimensional antiferromagnetic order becomes locally suppressed by Ga doping. The dilution of the spin lattice by nonmagnetic ions induces magnetic moments in triangular layers.<sup>24</sup> This increases magnetic susceptibility of the Mn layers and destroys the spin cancellation in triangles. Therefore, the local suppression of

the  $120^\circ$  spin ordering relieves the frustration and increases energy of the interlayer interaction, which can, in turn, lead to an enhancement of magnetoelectric coupling in the  $c$  direction. The proposed scenario is similar to the mechanism responsible for antiferromagnetic ordering induced by doping in the quasi-one-dimensional spin-Peierls material  $\text{CuGeO}_3$ ,<sup>25</sup> where the substitution of magnetic Cu by non-magnetic Zn or Mg breaks spin singlets in Cu chains and gives rise to a three-dimensional spin ordering.<sup>26,27</sup>

A similar enhancement of magnetocapacitance was found in Ti-doped yttrium manganite.<sup>28</sup> That material, however, shows a structural transition induced by Ti doping, whereas  $\text{YMn}_{1-x}\text{Ga}_x\text{O}_3$  remains hexagonal and ferroelectric for all doping concentrations considered, showing that the observed increase of magnetocapacitance in yttrium manganite is largely an effect of Ga substitution on the magnetic ordering.

In conclusion, Ga substitution in  $\text{YMnO}_3$  suppresses antiferromagnetic ordering and leads to a strong enhancement

of magnetocapacitance, which we ascribe to increased magnetic coupling between layers.

We thank B. Noheda, G. Catalan, and A. Meetsma for useful discussion. We thank J. Baas and N. Mufti for technical assistance. The work of A.A.N. is supported by the NWO Breedtestrategie Program of the Material Science Center, RuG, and by KNAW, Dutch Royal Academy of Sciences, through the SPIN Postdoc program. This work is in part supported by the Stichting FOM (Fundamental Research on Matter) and in part by the EU STREP program MaCoMuFi under Contract No. FP6-2004-NMP-TI-4 STRP 033221. M.M. gratefully acknowledges the support by the DFG (Mercator fellowship) and the hospitality of Cologne University. N.B. acknowledges financial support to SCOOTMO Research Training Network HPRN-CT-2002-00293, NOV-ELOX ESRT MEST-CT-2004-514237, and CNRS.

- 
- <sup>1</sup>T. T. M. Palstra and G. Blake, in *Encyclopedia of Materials: Science and Technology*, 2006 online update, edited by K. H. J. Buschow, H. C. Flemings, R. W. Cahn, P. Veysière, E. J. Kramer, and S. Mahajan (Elsevier, New York, 2006), www.sciencedirect.com
- <sup>2</sup>D. Fröhlich, St. Leute, V. V. Pavlov, and R. V. Pisarev, *Phys. Rev. Lett.* **81**, 3239 (1998).
- <sup>3</sup>M. Fiebig, Th. Lottermoser, D. Fröhlich, A. V. Goltsev, and R. V. Pisarev, *Nature (London)* **491**, 818 (2002).
- <sup>4</sup>Z. J. Huang, Y. Cao, Y. Y. Sun, Y. Y. Xue, and C. W. Chu, *Phys. Rev. B* **56**, 2623 (1997).
- <sup>5</sup>T. Katsufuji, S. Mori, M. Masaki, Y. Moritomo, N. Yamamoto, and H. Takagi, *Phys. Rev. B* **64**, 104419 (2001).
- <sup>6</sup>H. Sugie, N. Iwata, and K. Kohn, *J. Phys. Soc. Jpn.* **71**, 1558 (2002).
- <sup>7</sup>P. A. Sharma, J. S. Ahn, N. Hur, S. Park, Sung Baek Kim, Seongsu Lee, J.-G. Park, S. Guha, and S.-W. Cheong, *Phys. Rev. Lett.* **93**, 177202 (2004).
- <sup>8</sup>A. Munoz, J. A. Alonso, M. J. Martinez-Lope, M. T. Casais, J. L. Martinez, and M. T. Fernandez-Diaz, *Phys. Rev. B* **62**, 9498 (2000).
- <sup>9</sup>P. J. Brown and T. Chatterji, *J. Phys.: Condens. Matter* **18**, 10085 (2006).
- <sup>10</sup>T. Kimura, T. Goto, H. Shintani, K. Ishizaka, T. Arima, and Y. Tokura, *Nature (London)* **426**, 55 (2003).
- <sup>11</sup>T. Kimura, G. Lawes, T. Goto, Y. Tokura, and A. P. Ramirez, *Phys. Rev. B* **71**, 224425 (2005).
- <sup>12</sup>M. Kenzelmann, A. B. Harris, S. Jonas, C. Broholm, J. Schefer, S. B. Kim, C. L. Zhang, S.-W. Cheong, O. P. Vajk, and J. W. Lynn, *Phys. Rev. Lett.* **95**, 087206 (2005).
- <sup>13</sup>H. D. Zhou, J. C. Denyszyn, and J. B. Goodenough, *Phys. Rev. B* **72**, 224401 (2005).
- <sup>14</sup>U. Adem, A. A. Nugroho, A. Meetsma, and T. T. M. Palstra, *Phys. Rev. B* **75**, 014108 (2007).
- <sup>15</sup>B. B. Van Aken, T. T. M. Palstra, A. Filippetti, and N. A. Spaldin, *Nat. Mater.* **3**, 164 (2004).
- <sup>16</sup>Bas B. Van Aken and Thomas T. M. Palstra, *Phys. Rev. B* **69**, 134113 (2004).
- <sup>17</sup>Seongsu Lee, A. Pirogov, Jung Hoon Han, J.-G. Park, A. Hoshikawa, and T. Kamiyama, *Phys. Rev. B* **71**, 180413(R) (2005).
- <sup>18</sup>M. Doerr, M. Rotter, and A. Lindbaum, *Adv. Phys.* **54**, 1 (2005).
- <sup>19</sup>S. A. Kizhaev, V. A. Bokov, and O. V. Kachalov, *Sov. Phys. Solid State* **8**, 215 (1966).
- <sup>20</sup>B. Lorenz, A. P. Litvinchuk, M. M. Gospodinov, and C. W. Chu, *Phys. Rev. Lett.* **92**, 087204 (2004).
- <sup>21</sup>M. Campostrini, M. Hasenbusch, A. Pelissetto, P. Rossi, and Ettore Vicari, *Phys. Rev. B* **65**, 144520 (2002).
- <sup>22</sup>C.-G. Zhong and Q. Jiang, *J. Phys.: Condens. Matter* **14**, 8605 (2002).
- <sup>23</sup>C. delaCruz, F. Yen, B. Lorenz, Y. Q. Wang, Y. Y. Sun, M. M. Gospodinov, and C. W. Chu, *Phys. Rev. B* **71**, 060407(R) (2005).
- <sup>24</sup>A. Harrison, *J. Phys. C* **20**, 6287 (1987).
- <sup>25</sup>M. Hase, I. Terasaki, and K. Uchinokura, *Phys. Rev. Lett.* **70**, 3651 (1993).
- <sup>26</sup>D. Khomskii, W. Geertsma, and M. Mostovoy, *Czech. J. Phys.* **46**, 3229 (1996).
- <sup>27</sup>M. Mostovoy and D. Khomskii, *Z. Phys. B: Condens. Matter* **103**, 209 (1997).
- <sup>28</sup>Y. Aikawa, T. Katsufuji, T. Arima, and K. Kato, *Phys. Rev. B* **71**, 184418 (2005).